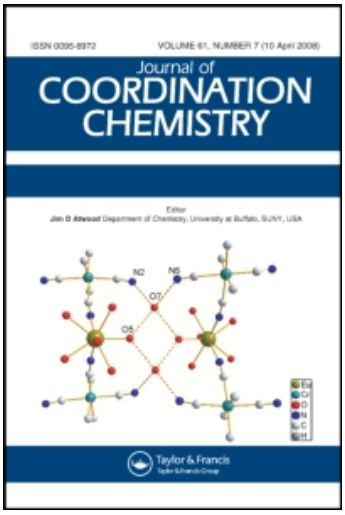

Journal of Coordination Chemistry
Publication details, including instructions for authors and subscription information:
http://www.informaworld.com/smpp/title~content=t713455674

Synthesis, characterization and crystal structure determination of iron(III) complexes containing 4,4'-dimethyl-2,2'-bipyridine, dimethyl sulfoxide and chloride, $[Fe(dmbipy)Cl_4][dmbipyH]$ and $[Fe(dmbipy)Cl_3(DMSO)]$

Vahid Amani[a]; Nasser Safari[a]; Behrouz Notash[a]; Hamid Reza Khavasi[a]
[a] Chemistry Department, Shahid Beheshti University, Tehran, Iran

To cite this Article Amani, Vahid , Safari, Nasser , Notash, Behrouz and Khavasi, Hamid Reza(2009) 'Synthesis, characterization and crystal structure determination of iron(III) complexes containing 4,4'-dimethyl-2,2'-bipyridine, dimethyl sulfoxide and chloride, $[Fe(dmbipy)Cl_4][dmbipyH]$ and $[Fe(dmbipy)Cl_3(DMSO)]$', Journal of Coordination Chemistry, 62: 12, 1939 — 1950
To link to this Article: DOI: 10.1080/00958970902736764
URL: http://dx.doi.org/10.1080/00958970902736764

Journal of Coordination Chemistry
Vol. 62, No. 12, 20 June 2009, 1939–1950

Taylor & Francis
Taylor & Francis Group

Synthesis, characterization and crystal structure determination of iron(III) complexes containing 4,4′-dimethyl-2,2′-bipyridine, dimethyl sulfoxide and chloride, [Fe(dmbipy)Cl_4][dmbipyH] and [Fe(dmbipy)Cl_3(DMSO)]

VAHID AMANI, NASSER SAFARI*, BEHROUZ NOTASH and HAMID REZA KHAVASI

Chemistry Department, Shahid Beheshti University, G. C., Tehran, Iran

(*Received 6 July 2008; in final form 19 September 2008*)

[Fe(dmbipy)Cl_4][dmbipyH], **1** (dmbipy is 4,4′-dimethyl-2,2′-bipyridine), was prepared from reaction of $FeCl_3 \cdot 6H_2O$ with 4,4′-dimethyl-2,2′-bipyridine in 0.1 molar aqueous HCl. Treatment of **1** with dimethyl sulfoxide in methanol produced [Fe(dmbipy)Cl_3(DMSO)], **2** (DMSO is dimethyl sulfoxide). Both complexes were characterized by IR, UV-vis, and ^{1}H-NMR spectroscopies and their structures were studied by single crystal diffraction. Compounds **1** and **2** are high-spin with spin multiplicity of six.

Keywords: Iron(III); 4,4′-Dimethyl-2,2′-bipyridine; Chloride; Dimethyl sulfoxide; Crystal structure

1. Introduction

Products formed by the reaction of iron(III) chloride with bidentate nitrogen donor ligands (L) like 1,10-phenanthroline (phen) and 2,2′-bipyridine (bipy) have been widely studied [1–11]. However, only a few of the resulting compounds such as $[Fe(L)_2Cl_2][FeCl_4]$ [12–14], $[FeCl_3(phen)X]$ [15] ($X = CH_3OH$, H_2O, Cl^-], $[Fe(bipy)_3][Cl_3FeOFeCl_3]$ [16], and $[Fe_2O(phen)_4Cl_2]Cl_2$ [16] have been fully characterized, in particular with the help of crystallographic studies. Owing to the lability of high-spin iron(III) species, few iron(III) complexes with three different ligands are known. We recently reported synthesis and crystal structure of [Fe(bipy)Cl_3][bipyH], $[Fe(dmbipy)_2Cl_2][FeCl_4]$ [17] (dmbipy is 5,5′-dimethyl-2,2′-bipyridine), [Fe(bipy)Cl_3(DMSO)], [Fe(phen)Cl_3(DMSO)] [18], and [Fe(phen)$Cl_3(CH_3OH)] \cdot CH_3OH$ [19].

*Corresponding author. Email: n-safari@cc.sbu.ac.ir

Journal of Coordination Chemistry
ISSN 0095-8972 print/ISSN 1029-0389 online © 2009 Taylor & Francis
DOI: 10.1080/00958970902736764

In this article we introduce a new complex, $[Fe^{III}(dmbipy)Cl_3(DMSO)]$, obtained from reaction of $[Fe^{III}(dmbipy)Cl_4]^-[dmbipyH]^+$ (dmbipy is 4,4′-dimethyl-2,2′-bipyridine) with DMSO in methanolic solution.

2. Experimental

2.1. *Materials and instruments*

All reagents and solvents were purchased from chemical sources and were used without purification. ^{1}H-NMR spectra were recorded on a Bruker AC-300 MHz spectrometer operating in the quarter mode. The spectra were collected over a 50-kHz bandwidth with 16 K data points and a 5-μs 45° pulse. For a typical spectrum, between 1000 and 5000 transients were accumulated with a 50-ms delay time. The signal-to-noise ratio was improved by apodization of the free induction decay. Infrared spectra (4000–250 cm^{-1}) of solid samples were taken as 1% dispersion in CsI pellets using a Shimadzu-470 spectrometer. UV-vis spectra were recorded on a Shimadzu 2100 spectrometer using a 1 cm path length cell. Melting point is uncorrected and was obtained by a Kofler Heizbank Rechart type 7841 melting point apparatus. Elemental analysis was performed using a Heraeus CHN–O rapid analyzer.

2.2. *Synthesis of [Fe(dmbipy)Cl$_4$][dmbipyH] (1)*

4,4′-Dimethyl-2,2′-bipyridine (0.30 g, 1.62 mmol) in 16.2 mL 0.1 M HCl was added to a solution of $FeCl_3 \cdot 6H_2O$ (0.22 g, 0.81 mmol) in water (5 mL) and the resulting red solution was stirred at 55–60°C for 3 h. The orange precipitate was recrystallized from CH_3CN. After three days, orange prismatic crystals of **1** were isolated (yield 0.34 g, 74.4%, m.p. 195°C). IR (CsI, cm^{-1}): 3432m, 3199w, 3058s, 2918m, 2851w ν(CH), 1620s, 1596s, 1550m, 1523m, 1483m, 1450s, 1412m, 1379w, 1308m, 1281m, 1246w, 1216m, 1112w, 1041w, 1016m, 999w, 943w, 904w, 826s, 756w, 738w, 658w, 549m, 522m, 468m, 422m, 302s ν(Fe–Cl), 288s ν(Fe–Cl), 255s ν(Fe–N). Anal. Calcd C, 50.78; H, 4.41; N, 9.87. Found: C, 50.61; H, 4.32; N, 9.73.

2.3. *Synthesis of [Fe(dmbipy)Cl$_3$(DMSO)] (2)*

DMSO (0.24 mL, 3.52 mmol) was added to a solution of [Fe(dmbipy)Cl_4][dmbipyH] (0.25 g, 0.44 mmol) in CH_3OH (30 mL) and the resulting orange solution was stirred at 40–45°C for 2 h. This solution was left to evaporate slowly at room temperature. After 1 week, yellow prismatic crystals of **2** were isolated (yield 0.14 g, 74.8%, decompose $<$189°C). IR (CsI, cm^{-1}): 3551w, 3468w, 3068m, 2998m, 2912m ν(CH), 1706m, 1613s, 1555m, 1485m, 1446m, 1406m, 1324w, 1303m, 1283w, 1240m, 1214w, 1021m, 983s, 947s, 923m, 841s, 739w, 718w, 549m, 522m, 447m, 424m ν(Fe–O), 388w, 346m, 308s ν(Fe–Cl), 282s ν(Fe–Cl), 256m ν(Fe–N). Anal. Calcd C, 39.57; H, 4.24; N, 6.59. Found: C, 39.41; H, 4.16; N, 6.43.

2.4. *Crystal structure determination and refinement*

The X-ray diffraction measurements were made on a STOE IPDS-II diffractometer with graphite monochromated Mo-Kα radiation. For [Fe(dmbipy)Cl_4][dmbipyH], **1**, an orange prismatic crystal with dimensions $0.20 \times 0.17 \times 0.10$ mm and for [Fe(dmbipy)Cl_3(DMSO)], **2**, a deep yellow prismatic crystal with dimensions $0.30 \times 0.30 \times 0.12$ mm were mounted on a glass fiber and used for data collection. Cell constants and an orientation matrix for data collection were obtained by least-squares refinement of diffraction data from 6802 for **1** and 4740 for **2** unique reflections. Data were collected at a temperature of 120(2) K to a maximum 2θ value of 58.48° for **1** and 58.46° for **2** in a series of ω scans in 1° oscillations and integrated using the Stoe X-AREA [20] software package. The numerical absorption coefficients, μ, for Mo-Kα radiation are 1.038 mm^{-1} for **1** and 1.425 mm^{-1} for **2**. A numerical absorption correction was applied using X-RED [21] and X-SHAPE [22] software. The data were corrected for Lorentz and polarization effects. The structures were solved by direct methods [23] and subsequent difference Fourier maps and then refined on F^2 by full-matrix least-squares using anisotropic displacement parameters [23]. All hydrogen atoms were located in a difference Fourier map and refined isotropically. Subsequent refinement converged with *R* factors and parameter errors significantly better than for all attempts to model the solvent disorder. Atomic factors are from International Tables for X-ray Crystallography [24]. All refinements were performed using the X-STEP32 crystallographic software package [25]. A summary of the crystal data, experimental details, and refinement results is given in table 1.

3. Results and discussion

3.1. *Synthesis of [Fe(dmbipy)Cl_4][dmbipyH] (1) and [Fe(dmbipy)Cl_3(DMSO)] (2)*

Compound **1** was obtained from reaction of one equivalent of $FeCl_3 \cdot 6H_2O$ with 2 equivalents of 4,4′-dimethyl-2,2′-bipyridine in 0.1 M HCl aqueous solution at 55°C for 3 h, in 74% yield, equation (1):

$$FeCl_3 \cdot 6H_2O + 2\text{dmbipy} \xrightarrow[H_2O,\ HCl\ 0.1\ M]{55-60^\circ C,\ 3\ h} [\text{Fe(dmbipy)}Cl_4][\text{dmbipyH}] \quad (1)$$

Coordination of iron(II) with 4,4′-dimethyl-2,2′-bipyridine leads to the highly stable *tris*-dmbipy complexes, $[\text{Fe(dmbipy)}_3](ClO_4)_2 \cdot H_2O$ [26] and $[\text{Fe(dmbipy)}_3](SCN)_2 \cdot 3H_2O$ [27]. However, the *bis*-iron(III) complex $[\text{Fe(dmbipy)}_2Cl_2]PF_6$ [28] has been reported. Here, the aqueous HCl solution is a driving force for formation of **1** in which only one dmbipy coordinates iron and the other is a counter ion with abstraction of proton from the acidic environment.

Addition of DMSO to methanolic solution of **1** results in formation of **2**, equation (2), in which one chloride is exchanged by DMSO.

$$[\text{Fe(dmbipy)}Cl_4][\text{dmbipyH}] \xrightarrow[CH_3OH/DMSO]{40-45^\circ C,\ 2\ h} [\text{Fe(dmbipy)}Cl_3(\text{DMSO})] + \text{dmbipyHCl} \quad (2)$$

Table 1. Crystallographic and structure refinements data for **1** and **2**.

	1	**2**
Formula	$C_{24}H_{25}C_{l4}FeN_4$	$C_{14}H_{18}Cl_3FeN_2OS$
Formula weight	567.13	424.57
Temperature (K)	120(2)	120(2)
Wavelength λ (Å)	0.71073	0.71073
Crystal system	Monoclinic	Monoclinic
Space group	$P2_1/c$	$P2_1/n$
Crystal size (mm^3)	$0.20 \times 0.17 \times 0.10$	$0.30 \times 0.30 \times 0.12$
Units of dimensions (Å, °)		
a	10.8567(6)	8.0916(5)
b	10.4776(7)	22.8995(13)
c	22.5132(13)	9.8841(7)
β	98.511(4)	105.136(5)
Volume ($Å^3$)	2532.7(3)	1767.92(19)
Z	4	4
Density (Calcd) ($g\,cm^{-1}$)	1.487	1.595
θ ranges for data collection	1.83–29.24	1.78–29.23
F(000)	1164	868
Absorption coefficient (mm^{-1})	1.038	1.425
Index ranges	$-12 \le h \le 14$ $-14 \le k \le 12$ $-30 \le l \le 30$	$-11 \le h \le 11$ $-31 \le k \le 30$ $-13 \le l \le 12$
Data collected	17676	13,282
Unique data (R_{int})	6802 (0.0775)	4740 (0.0254)
Parameters, restraints	302, 0	202, 0
Final R_1, wR_2[a] (Obs. data)	0.0548, 0.1282	0.0317, 0.0750
Final R_1, wR_2[a] (all data)	0.0667, 0.1346	0.0347, 0.0763
Goodness-of-fit on F^2 (*S*)	1.127	1.127
Largest differential peak and hole ($e\,Å^{-3}$)	0.899, −0.673	0.589, −0.704

[a] $R_1 = \Sigma||F_o|-|F_c||/\Sigma|F_o|$, $wR_2 = [\Sigma(w(F_o^2 - F_c^2)^2)/\Sigma w(F_o^2)^2]^{1/2}$.

Compound **1** and analogs with general formula of $[Fe(N–N)Cl_4]^-[N–N \cdot H]^+$ (N–N is 1,10-phenanthroline, 2,2′-bipyridine, and 4,4′-dimethyl-2,2′-bipyridine) are excellent precursors for production of neutral high-spin iron(III) complexes of $[Fe^{III}(N–N)Cl_3(D)]$ formula, where D is a donor ligand. Using this approach, compounds such as $[Fe(bipy)Cl_3(DMSO)]$, $[Fe(phen)Cl_3(DMSO)]$ [18], and $[Fe(phen)Cl_3(CH_3OH)] \cdot CH_3OH$ [19] were previously prepared. The Fe–Cl bond distances in **1** indicate that one Fe–Cl bond is longer than the others due to hydrogen bond formation with the cationic part of the complex, table 4; this chloride was easily removed by any basic solvent or ligand.

A similar approach to $[Fe(N–N)Cl_4]^-[N–N–H]^+$ resulted in different compounds, depending on the bipyridine used, equations 3–5. The structure of bipyridine and its analogs were optimized at B3LYP/6–31G* level optimization and as recommended in Gaussian help, point charge of all species have been obtained from a HF/6–31G* single point calculation in *gauss 03* using ESP based procedure. Table 2 shows 6–31G* *ab initio* calculation results for charge densities on nitrogens of the bipyridine analogs. More basic character of the nitrogens of N–N ligands produces stronger N–H bonds in the cationic part of the complexes and reduces the affinity of bipyridine analogs for coordination to the iron. So in bipy and 4,4′-dimethyl-2,2′-bipyridine there is one chelating ligand in coordination atmosphere, while for

Table 2. HF/6–31G*//B3LYP/6–31G* calculation using ESP-based procedure for charge densities on nitrogens of the bipyridine analogs.

Compound	Nitrogen atom
Bipyridine	−0.661
4,4′-Dimethyl-2,2′-bipyridine	−0.669
	−0.729
5,5′-Dimethyl-2,2′-bipyridine	−0.644
	−0.618

5,5′-dimethyl-2,2′-bipyridine, which is less basic, is coordinated to the iron. Steric hindrance in methyl substituted bipy ligands shows no effect in this regard and crystal structures reveal no hindrance for these complexes.

$$FeCl_3 \cdot 6H_2O + 2(4,4' - dmbipyHCl) \rightarrow [Fe(4,4' - dmbipy)Cl_4][4,4' - dmbipyH] \quad (3)$$

$$FeCl_3 \cdot 6H_2O + 2(bipyHCl) \rightarrow [Fe(bipy)Cl_4][bipyH] \quad (4)$$

$$FeCl_3 \cdot 6H_2O + 2(5,5' - dmbipyHCl) \rightarrow [Fe(5,5'-dmbipy)_2Cl_2][FeCl_4] \quad (5)$$

3.2. *^{1}H NMR investigation*

Paramagnetic ^{1}H-NMR of some bipyridine and phenanthroline iron complexes show coordinated methanol protons around 100 ppm downfield, DMSO protons at 40 ppm and coordinated bipyridine or phenanthroline protons in the 6–9 ppm region. ^{1}H-NMR of **1** and **2** are presented in Supplementary Material. The spectrum of **1** right away after dissolution in 99.8% CD_3OD shows coordinated CH_3OH as a broad signal at 100 ppm and 4-methyl of bipyridine at 20 ppm. This spectrum shows exchange of CH_3OH with chloride in the methanolic solution as a fast process giving [Fe(dmbipy)Cl_3(CH_3OH)], **3**. Addition of a 30 mole ratio of DMSO to the methanolic solution of **1** shows a major broad peak at 40 ppm. The methyl of dmbipy for **2** and **3** are seen at 20 ppm. Trace C is a pure sample of **2** dissolved in methanol and confirms the presence of **2** and **3** due to lability of DMSO in methanolic solution as expected for high-spin Fe(III) complexes. The NMR shows that the plane of symmetry for **2** or **3** in the solid state passing through carbon of DMSO or methanol, Fe and Cl_3 still holds in solution. The similar chemical shifts for methyl protons of DMSO, methyl protons on 4,4′-dimethyl-2,2′-bipyridine, and three separate signals for protons on coordinated bipyridine are attributed to this symmetry element. Protons on the 6 and 6′ positions, closest to iron, are broadest signals at 8–9 ppm. However, proton signals for other bipy protons in the equatorial position have small bandwidth compared to protons of methanol or DMSO at the axial position. It seems the dominant mechanism for spin transfer is dipolar for axial position and contact for equatorial protons.

Magnetic susceptibility measurements for **1** and **2** by Evans method confirm the high-spin character of these complexes ($\mu_{eff} = 5.8$ B.M) [29].

3.3. *IR and UV-vis investigation*

IR absorptions of the free ligands and **1** and **2** are presented in table 3. Two strong bands in **1** at 302 and 288 cm^{-1} were assigned to Fe–Cl and the band at 255 cm^{-1} to Fe–N based on literature reports [30, 31]. Fe–N stretching vibration for **2** is at 256 cm^{-1} and Fe–Cl at 308 and 282 cm^{-1}. A new signal at 983 cm^{-1} for **2** is assigned to υ(S=O). Other iron(III) DMSO complexes reported in the literature have υ(S=O) in the 910–960 cm^{-1} region [32]. The band at 424 cm^{-1} was assigned to Fe–O stretch in **2** [32].

UV-vis spectra of **1**–**3** (Supplementary Material) lack spin allowed d–d transitions in the visible region, but have distinct charge transfer spectra in the UV region. Intensities of low-energy bands increase upon coordination of oxygen donors.

3.4. *Description of the molecular structure of [Fe(dmbipy)Cl_4][dmbipyH] (1) and [Fe(dmbipy)Cl_3(DMSO)] (2)*

Orange prismatic crystals of **1** were obtained by recrystallization of micro crystals of **1** in CH_3CN and yellow prismatic crystals of **2** were obtained by recrystallization of micro crystals of **1** in DMSO and CH_3OH. Crystallographic data for **1** and **2** are given in table 1 and selected bond lengths and angles are presented in table 4. The structure of **1** consists of $[Fe(dmbipy)Cl_4]^-$ anion and protonated dimethylbipyridine cation, figure 1. The iron(III) environment consists of four chlorides and one dimethylbipyridine, giving a distorted octahedral geometry. The different bond length values of the Fe(1)–Cl bonds *trans* to Cl and those *trans* to N (dmbipy), accompanied with the short bite angle of dmbipy [74.65(9)° for N(1)–Fe(1)–N(2)], are the main factors accounting for this distortion. The Fe–N (dmbipy) average bond distance is 2.184(1) Å and the Fe–Cl average bond distance is 2.3552(7) Å. These bond distances are longer than those observed for similar low-spin complexes [33]. The longer bond distance in **1** confirms that this complex is high-spin with $S = 5/2$, in accord with data obtained by magnetic moment measurements. Good agreement is observed between the Fe–Cl bond distances of **1** and those reported for other chloro-containing mononuclear high-spin iron(III) complexes [17–19, 34]. The unit cell-packing diagram of **1** is presented in figure 2. From this packing diagram, the intermolecular bond distances and angles for N–H···Cl (H···Cl = 2.4500(5)° and N–H···Cl = 145.00(6)°) confirm hydrogen bond formation between the counter ions. These intermolecular hydrogen bonds seem to be effective in stabilization of the crystal structure. The Fe(1)–Cl(1) bond distance is longer than the others (table 4) due to hydrogen bonding with the counter ion, making it more labile.

The crystal structure of **2** consists of three chlorides, one chelating dimethylbipyridine and one DMSO. ORTEP view with numbering scheme and packing diagram for **2** are shown in figures 3 and 4, respectively. This complex has distorted octahedral geometry. The different coordinated ligands, different bond distances for chloride *cis*, and *trans* relative to diimine are main factors accounting for these distortions, table 4. Fe–N average distance for **2** is 2.186(2) Å and the Fe–Cl average bond distance is 2.3088(5) Å. DMSO is coordinated to Fe(III) from the oxygen with Fe–O bond distance of 2.070(1) Å.

Metal–ligand bond lengths were used to obtain the spin state of the metal center, table 5. The Fe–N average bond distances in high-spin iron(III) phenanthroline and bipyridine complexes are 2.2 Å in high-spin complexes and less than 2 Å in low-spin

Table 3. Selected IR frequencies (cm^{-1}) of dmbipyridine, dimethyl sulfoxide and **1** and **2**.

Compound	υ(C=C), υ(C=N)	υ(ring deformation)	υ(C–H)	υ(Fe–N)	υ(S=O)	υ(Fe–Cl)	υ(Fe–O)
Dmbipy	1436, 1458, 1555, 1592	518, 670, 824, 912	3056	–	–	–	–
DMSO	–	–	2913, 2996	–	1050	–	–
[Fe(dmbipy)Cl_4] [dmbipyH]	1450, 1483, 1596, 1620	658, 738, 756, 826, 943	2918, 3058	255	–	288, 302	–
[Fe(dmbipy)Cl_3 (DMSO)]	1485, 1555, 1613, 1706	549, 718, 739, 841, 923	2912, 2998, 3068	256	983	308, 282	424

Table 4. Selected bond distances (Å) and angles (°) for **1** and **2**.

1			
Fe(1)–N(1)	2.191(2)	N(1)–Fe(1)–Cl(4)	168.46(7)
Fe(1)–N(2)	2.176(2)	Cl(2)–Fe(1)–Cl(4)	98.28(3)
Fe(1)–Cl(1)	2.424(1)	N(2)–Fe(1)–Cl(3)	85.84(6)
Fe(1)–Cl(2)	2.314(1)	N(1)–Fe(1)–Cl(3)	88.00(6)
Fe(1)–Cl(3)	2.364(1)	Cl(2)–Fe(1)–Cl(3)	95.25(3)
Fe(1)–Cl(4)	2.319(1)	Cl(4)–Fe(1)–Cl(3)	94.24(3)
N(3)–H(3)	0.81(4)	N(2)–Fe(1)–Cl(1)	84.67(6)
N(2)–Fe(1)–N(1)	74.65(9)	N(1)–Fe(1)–Cl(1)	84.71(6)
N(2)–Fe(1)–Cl(2)	167.35(6)	Cl(2)–Fe(1)–Cl(1)	92.94(3)
N(1)–Fe(1)–Cl(2)	92.78(7)	Cl(4)–Fe(1)–Cl(1)	91.40(3)
N(2)–Fe(1)–Cl(4)	94.20(6)	Cl(3)–Fe(1)–Cl(1)	169.29(3)
2			
Fe(1)–N(1)	2.181(2)	O(1)–Fe(1)–Cl(2)	90.46(4)
Fe(1)–N(2)	2.190(2)	N(1)–Fe(1)–Cl(2)	168.30(4)
Fe(1)–O(1)	2.070(1)	N(2)–Fe(1)–Cl(2)	95.18(4)
Fe(1)–Cl(1)	2.290(1)	Cl(1)–Fe(1)–Cl(2)	96.269(18)
Fe(1)–Cl(2)	2.307(1)	O(1)–Fe(1)–Cl(3)	167.91(4)
Fe(1)–Cl(3)	2.329(1)	N(1)–Fe(1)–Cl(3)	88.92(4)
S(1)–O(1)–Fe(1)	122.73(8)	N(2)–Fe(1)–Cl(3)	87.97(4)
O(1)–Fe(1)–N(1)	83.60(5)	Cl(1)–Fe(1)–Cl(3)	98.27(2)
O(1)–Fe(1)–N(2)	80.85(5)	Cl(2)–Fe(1)–Cl(3)	95.147(18)
N(1)–Fe(1)–N(2)	73.97(6)	O(1)–S(1)–C(13)	102.49(9)
O(1)–Fe(1)–Cl(1)	91.74(4)	O(1)–S(1)–C(14)	105.22(9)
N(1)–Fe(1)–Cl(1)	93.99(4)	C(13)–S(1)–C(14)	98.75(10)
N(2)–Fe(1)–Cl(1)	166.40(4)		

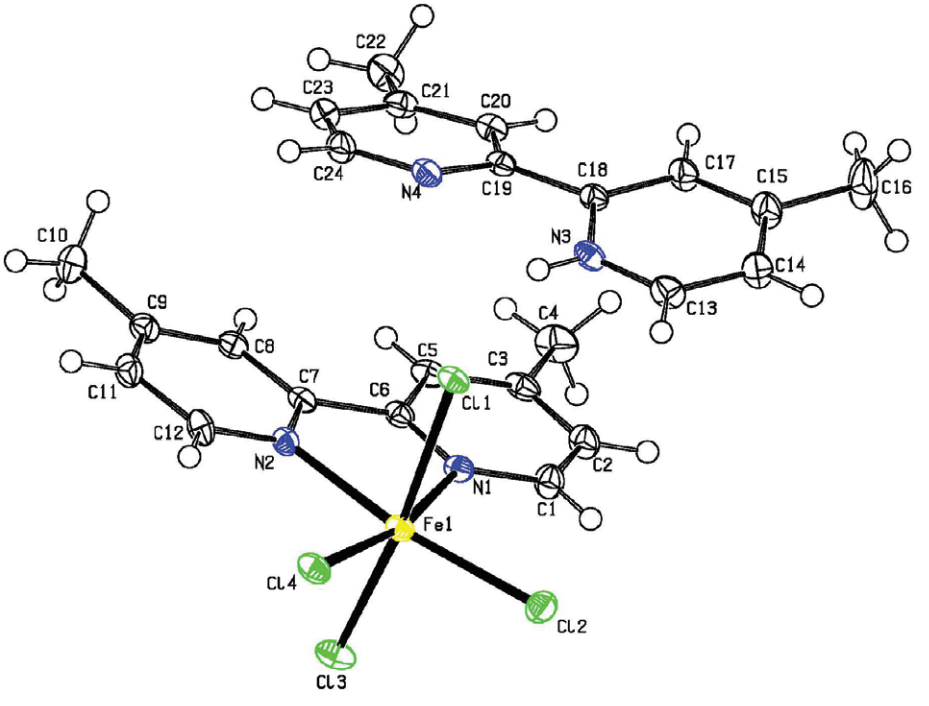

Figure 1. The labeled diagram of [Fe(dmbipy)Cl_4][dmbipyH] (**1**). Thermal ellipsoids are at 50% probability.

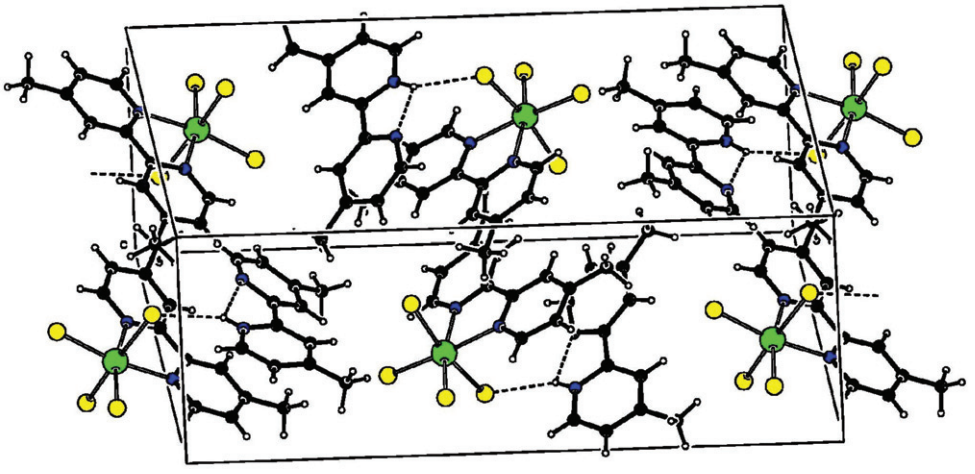

Figure 2. Crystal packing diagram for **1**. Hydrogen bonds are shown as dashed lines.

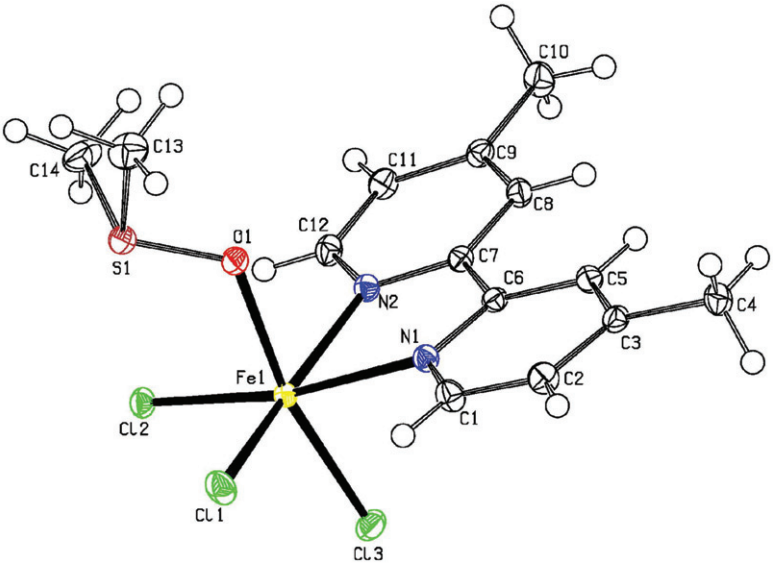

Figure 3. The labeled diagram of [Fe(dmbipy)Cl_3(DMSO)] (**2**). Thermal ellipsoids are at 50% probability.

Fe^{III} complexes [13, 34]. Therefore, the Fe–N bond distances here show the present complexes are high-spin d^5. The Fe–O bond distance for **2** is 2.070(1) Å, considerably shorter than in [Fe^{III}(phen)Cl_3(H_2O)] and [Fe^{III}(phen)Cl_3(CH_3OH)] · CH_3OH (2.19 and 2.137 Å, respectively). Elongation is due to hydrogen bond formation observed in [Fe^{III}(phen)Cl_3(H_2O)] and [Fe^{III}(phen)Cl_3(CH_3OH)] · CH_3OH. The Fe–O bond distance in **2** is similar to [Fe^{III}(phen)Cl_3(DMSO)] and [Fe^{III}(bipy)Cl_3(DMSO)] [18] with no hydrogen bonding.

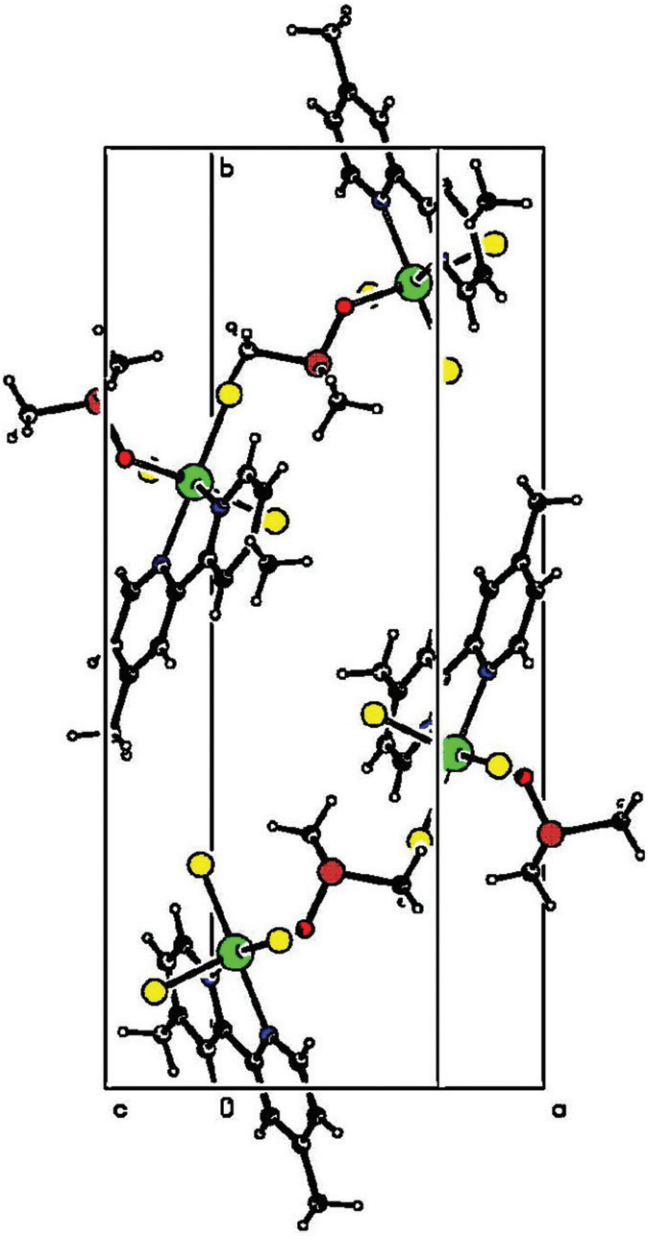

Figure 4. Crystal packing diagram for **2**.

Supplementary material

Full crystallographic details are deposited with Cambridge Structural Database (CCDC No. 679538 for **1** and 679539 for **2**). Copies of the data can be obtained free of charge on application to CCDC, 12 Union Road, Cambridge CB2 1EZ, UK.

Table 5. The mean bond distances (Å) and angles (°) of some phenanthroline, bipyridine, and dmbipyridine iron(III) complexes.

Iron complex	⟨Fe–N⟩ (Å)	⟨Fe–Cl⟩ (Å)[a]	⟨Fe–Cl⟩ (Å)[b]	N–Fe–N angle (°)	Spin-state	Reference
$[Fe(phen)Cl_4]^-$	2.201(1)	2.320(2)	2.382(1)	75.04(6)	H.S.	[35]
$[Fe(bipy)Cl_4]^-$	2.193(3)	2.392(1)	2.299(1)	73.91(1)	H.S.	[17]
$[Fe(dmbipy)Cl_4]^-$	2.184(1)	2.317(2)	2.394(1)	74.65(9)	H.S.	Present work
$[Fe(bipy)Cl_3(DMSO)]$	2.187(14)	2.309(6)	2.305(1)	74.17(6)	H.S.	[18]
$[Fe(dmbipy)Cl_3(DMSO)]$	2.186(2)	2.299(2)	2.329(1)	73.97(6)	H.S.	Present work
$[Fe(phen)Cl_3(DMSO)]$	2.213(2)	2.294(8)	2.342(1)	75.49(8)	H.S.	[18]
$[Fe(phen)Cl_3(H_2O)]$	2.174(3)	2.266(1)	2.342(1)	75.6(1)	H.S.	[34]
$[Fe(phen)Cl_3(CH_3OH)]$	2.187(3)	2.288(1)	2.302(2)	74.60(10)	H.S.	[19]
$[Fe(phen)_2Cl_2]$	2.222(3)	2.415(11)	–	–	H.S.	[36]
$[Fe(dmbipy)_2Cl_2]^+$	2.167(1)	2.651(6)	–	75.615(6)	H.S.	[28]
$[Fe(bipy)_3]^{2+}$	1.965(3)	–	–	83.196(16)	L.S.	[37]
$[Fe(dmbipy)_3]^{2+}$	1.965(3)	–	–	81.30(13)	L.S.	[27]
$[Fe(phen)_3]^{2+}$	1.974(3)	–	–	82.976(12)	L.S.	[38]
$[Fe(phen)_3]^{3+}$	1.976(1)	–	–	82.43(6)	L.S.	[39]

Note: [a]Equatorial.
[b]Axial.

Acknowledgments

We would like to thank the Iranian National Science Foundation and Research and Graduate Study Councils of Shahid Beheshti University for financial support.

References

[1] A. Gaines, L.P. Hammett, G.H. Walden. *J. Am. Chem. Soc.*, **58**, 1668 (1936).
[2] A. Simon, G. Morgenstern, W.H.Z. Albrecht. *Anorg. Allg. Chem.*, **230**, 225 (1937).
[3] L. Michaelis, S. Granick. *J. Am. Chem. Soc.*, **65**, 481 (1943).
[4] H. Irving, E.J. Buttler, M.F. King. *J. Chem. Soc.*, 1489 (1949).
[5] C.M. Harris, T.N. Lockyer. *Chem. Ind. (London)*, 1231 (1958).
[6] A. Earnshaw, J. Lewis. *J. Chem. Soc.*, 396 (1961).
[7] G. Anderegg. *Helv. Chim. Acta*, **45**, 1643 (1962).
[8] B.N. Figgis, J. Lewis. *Prog. Inorg. Chem.*, **6**, 168 (1964).
[9] A.V. Khedekar, J. Lewis, F.E. Mabbs, H. Weigold. *J. Chem. Soc., A*, 1561 (1967).
[10] R.R. Berrett, B.W. Fitzsimmons, A.A. Owusu. *J. Chem. Soc., A*, 1575 (1968).
[11] S.N. Ghosh. *Indian J. Chem.*, **13**, 66 (1975).
[12] H.J. Goodwin, M. Mc Partlin, H.A. Goodwin. *Inorg. Chim. Acta*, **25**, L74 (1977).
[13] B.N. Figgis, J.M. Patrick, P.A. Reynolds, B.W. Skelton, A.H. White, P.C. Healy. *Aust. J. Chem.*, **36**, 2043 (1983).
[14] E.H. Witten, W.M. Rei, K. Lazar, B.W. Sullivan, B.M. Foxman. *Inorg. Chem.*, **24**, 4585 (1985).
[15] P.C. Healy, J.M. Patrick, B.W. Skelton, A.H. White. *Aust. J. Chem.*, **36**, 2031 (1983).
[16] P.C. Healy, B.W. Skelton, A.H. White. *Aust. J. Chem.*, **36**, 2057 (1983).
[17] V. Amani, N. Safari, H.R. Khavasi. *Polyhedron*, **26**, 4257 (2007).
[18] V. Amani, N. Safari, H.R. Khavasi, P. Mirzaei. *Polyhedron*, **26**, 4908 (2007).
[19] H.R. Khavasi, V. Amani, N. Safari. *Z. Kristallogr.*, **222**, 155 (2007).
[20] Stoe & Cie, X–AREA, vesion 1.30: Program for the acquisition and analysis of data, Stoe & Cie GmbH: Darmstadt, Germany (2005).
[21] Stoe & Cie, X–RED, vesion 1.28b: Program for data reduction and absorption correction, Stoe & Cie GmbH: Darmstadt, Germany (2005).
[22] Stoe & Cie, X–SHAPE, version 2.05: Program for crystal optimization for numerical absorption correction, Stoe & Cie GmbH: Darmstadt, Germany (2004).

[23] G.M. Sheldrick. SHELX97. Program for crystal structure solution and refinement, University of Göttingen, Germany (1997).
[24] International Tables for X-ray Crystallography, Vol. C, Kluwer Academic Publisher, Dordrecht, The Netherlands (1995).
[25] Stoe & Cie, X-STEP32, Version 1.07b: Crystallographic package; Stoe & Cie GmbH, Darmstadt, Germany (2000).
[26] W. Huang, H. Qian. *Transition Met. Chem.*, **31**, 621 (2006).
[27] W. Huang, T. Ogawa. *J. Mol. Struct.*, **785**, 21 (2006).
[28] M.-N. Collomb, A. Deronzier, K. Gorgy, J.-C. Leprêtre, J. Pécaut. *New J. Chem.*, **23**, 785 (1999).
[29] D.F. Evans. *J. Chem. Soc.*, 2003 (1959).
[30] Y. Saito, J. Takemoto, B. Hutchinson, K. Nakamoto. *Inorg. Chem.*, **11**, 2003 (1972).
[31] W.M. Reipf, B. Dockum, M.A. Weber, R.B. Frankel. *Inorg. Chem.*, **14**, 800 (1975).
[32] K. Nakamato. *Infrared and Raman Spectra of Inorganic and Coordination Compounds: Part B*, 5th Edn, Wiley, New York (1997).
[33] R.D. Poulsen, A. Hazell. *Acta Crystallogr., Sect. E*, **57**, m186 (2001).
[34] P. Kulkarni, S. Padhye, E. Sinn. *Polyhedron*, **17**, 2623 (1998).
[35] H.R. Khavasi, V. Amani, N. Safari. *Z. Kristallogr.*, **223**, 41 (2008).
[36] X.-C. Fu, M.-T. Li, C.-G. Wang. *Acta Crystallogr., Sect. E*, **61**, m1221 (2005).
[37] S.R. Batten, K.S. Murray, N.J. Sinclair. *Acta Crystallogr., Sect. C*, **56**, e320 (2000).
[38] L.A. Plaza, K. Baranowska, B. Becker. *Acta Crystallogr., Sect. E*, **63**, m1537 (2007).
[39] M. Odoko, N. Okabe. *Acta Crystallogr., Sect. E*, **60**, m1822 (2004).